Meteorol Atmos Phys (2018) 130:635–647
https://doi.org/10.1007/s00703-017-0542-9

ORIGINAL PAPER

WRF model for precipitation simulation and its application in real-time flood forecasting in the Jinshajiang River Basin, China

Jianzhong Zhou[1,2] · Hairong Zhang[1,2] · Jianyun Zhang[3] · Xiaofan Zeng[1,2] · Lei Ye[4] · Yi Liu[1,2] · Muhammad Tayyab[1,2] · Yufan Chen[5]

Received: 19 September 2016 / Accepted: 23 June 2017 / Published online: 13 July 2017

Abstract An accurate flood forecasting with long lead time can be of great value for flood prevention and utilization. This paper develops a one-way coupled hydro-meteorological modeling system consisting of the mesoscale numerical weather model Weather Research and Forecasting (WRF) model and the Chinese Xinanjiang hydrological model to extend flood forecasting lead time in the Jinshajiang River Basin, which is the largest hydropower base in China. Focusing on four typical precipitation events includes: first, the combinations and mode structures of parameterization schemes of WRF suitable for simulating precipitation in the Jinshajiang River Basin were investigated. Then, the Xinanjiang model was established after calibration and validation to make up the hydro-meteorological system. It was found that the selection of the cloud microphysics scheme and boundary layer scheme has a great impact on precipitation simulation, and only a proper combination of the two schemes could yield accurate simulation effects in the Jinshajiang River Basin and the hydro-meteorological system can provide instructive flood forecasts with long lead time. On the whole, the one-way coupled hydro-meteorological model could be used for precipitation simulation and flood prediction in the Jinshajiang River Basin because of its relatively high precision and long lead time.

Responsible Editor: M. Kaplan.

✉ Hairong Zhang
zhr@hust.edu.cn

Jianzhong Zhou
jz.zhou@hust.edu.cn

[1] School of Hydropower and Information Engineering, Huazhong University of Science and Technology, Wuhan 430074, China

[2] Hubei Key Laboratory of Digital Valley Science and Technology, Wuhan 430074, China

[3] State Key Laboratory of Hydrology-Water Resources and Hydraulic Engineering, Nanjing Hydraulic Research Institute, Nanjing 210098, China

[4] School of Hydraulic Engineering, Dalian University of Technology, Dalian 116024, China

[5] China Yangtze Power Company Limited, Yichang 443002, China

1 Introduction

Flooding is one of the most frequent and damaging natural disasters responsible for human deaths and economic loss. Approximately two-thirds of China are still currently under the threat of flooding to various degrees. Flood forecasts can provide the early warnings that are helpful in flood prevention, disaster relief, and public safety. Nowadays, flood forecasts mainly focus on land surface infiltration, flood generation, and routing. Although some achievements have been made, there are still some limitations in precision and forecasting lead time.

Precipitation, as an input for hydrological models, is the most important factor for flood forecasting. An accurate precipitation forecast can be of great value for increasing flood lead time and accuracy. Without a precipitation forecast, the flood forecasting lead time is thus limited to the natural flow concentration time of the basin, which is usually very short for practical use in hazard warning. High-resolution regional atmospheric models offer promising quantitative precipitation forecast, thus providing a helpful way to produce accurate and long lead time forecasts for the authorities in operational flood

management decision-making. A complete flood should contain precipitation process and hydrology process as a whole. That is why there are more and more studies attempting to take the precipitation forecast as the input of flood forecast model and build an atmospheric-hydrological coupled model.

The Weather Research and Forecasting (WRF) model, known as a next-generation mesoscale numerical weather prediction model, offers a flexible and computationally efficient platform for operational forecasting, taking advantage from recent advances in physics and numeric. It proved to be a useful tool in precipitation forecast and has proved to achieve some good results (Hong et al. 2004; Srivastava et al. 2015). In recent years, many researchers around the world have begun studying parameterization schemes for a mesoscale numerical weather predication system (Gilliam and Pleim 2010; Raju et al. 2011; Zeng et al. 2011; Yuan et al. 2012). The results have shown that the selection of parameterization schemes for the mesoscale numerical model has a significant impact on the results of precipitation simulation and prediction, and different regions require different parameterization schemes. Therefore, the selection of parameterization schemes and their combinations should be based on the conditions of the specific region (Yuan et al. 2012; Deb et al. 2008).

Compared with the distributed hydrological model, the lumped hydrological model is widely used, because it has a simple structure and needs fewer historical data and its parameter can be estimated more easily. However, when it comes to a basin with a large span of space, it should be divided into sub-basins based on its precipitation–runoff characteristics and the DEM data, and then establish a flood forecast system from upstream to downstream in the Basin. For each sub-basin, a conceptual hydrological model is built after calibration and validation using the observed precipitation and runoff data. Furthermore, with an instructive precipitation forecast (such as WRF model) as the input of flood forecast system, a flood forecast with high precision and long lead time can be obtained, thus providing beneficial information for scheduling and utilization of the water resources in the basin and ensuring the safety of people's life and property.

In this study, the Jinshajiang River Basin was used as the study area. First, the impact of various parameterization scheme combinations on different physical processes in the WRF model was investigated. The nesting mode configuration was also analyzed to select a suitable computational framework and parameterization scheme for the WRF model. Second, the Xinanjiang model was brought herein as the hydrological model. The Jinshajiang River Basin was divided into several sub-basins and a forecasting system was built by establishing the Xinanjiang model in every sub-basin. The outlet flood forecasts can be obtained through the forecasting system using the WRF's precipitation as input. At last, a one-way coupled hydro-meteorological system was built to generate precipitation and flood forecasts in real-time for the specified precipitation and flood events.

The structure of the paper is as follows: Sect. 2 introduces the study area and the selected data; Sect. 3 introduces research methods (including the experimental scheme design of the WRF model, the Xinanjiang model, and the flood forecast system); experimental scheme results of the WRF model, performance of the hydrological model, and precision of the one-way coupled hydro-meteorological system are given in Sect. 4; discussion and conclusion are demonstrated in Sect. 5.

2 Study area and data

2.1 Study area

Located in the upper reaches of the Yangtze River Basin, the Jinshajiang River Basin is situated in the Qinghai–Tibet Plateau, the Yunnan–Guizhou Plateau, and the western margin of the Sichuan Basin. It has a catchment area of 470,000 km^2, and the main river of the Jinshajiang River has a length of 3496 km (from the source to Yibin, Sichuan). The Jinshajiang River flows through five terrain units, including the Qinghai–Tibet Plateau, the western Sichuan Plateau, the Hengduan Mountains, the Yunnan–Guizhou Plateau, and the mountainous area of southwest Sichuan. The landforms and the topographical patterns of the Jinshajiang River Basin are extremely complicated, with the terrain showing a dramatic elevating trend from the southeast to northwest (Wu et al. 2011). The north and the northwest of the Jinshajiang River Basin are vast plateaus, while the south and the southeast are canyons, which have a relative relief of 1000–3000 m.

There are various climate types in the basin, which include typical plateau climates, stereoscopic climates, and monsoon climates. The Jinshajiang River Basin is a vulnerable region in terms of climate change and is relatively sensitive to climate change within the Yangtze River Basin. In addition to a dramatic spatio temporal climate change, there is a significant vertical difference in the basin (He et al. 2013). In the winter half year (October through May for the northern section of the Hengduan Mountains; November through April for the remainder of the basin), the Jinshajiang River Basin is mostly influenced by the westerly air current, which is divided by the Qinghai–Tibet Plateau into a north and south jet stream. The southern flow passes through the Yunnan–Guizhou Plateau and creates continental, sunny, and dry weather for the basin. However, the northeast region of the basin is influenced by the

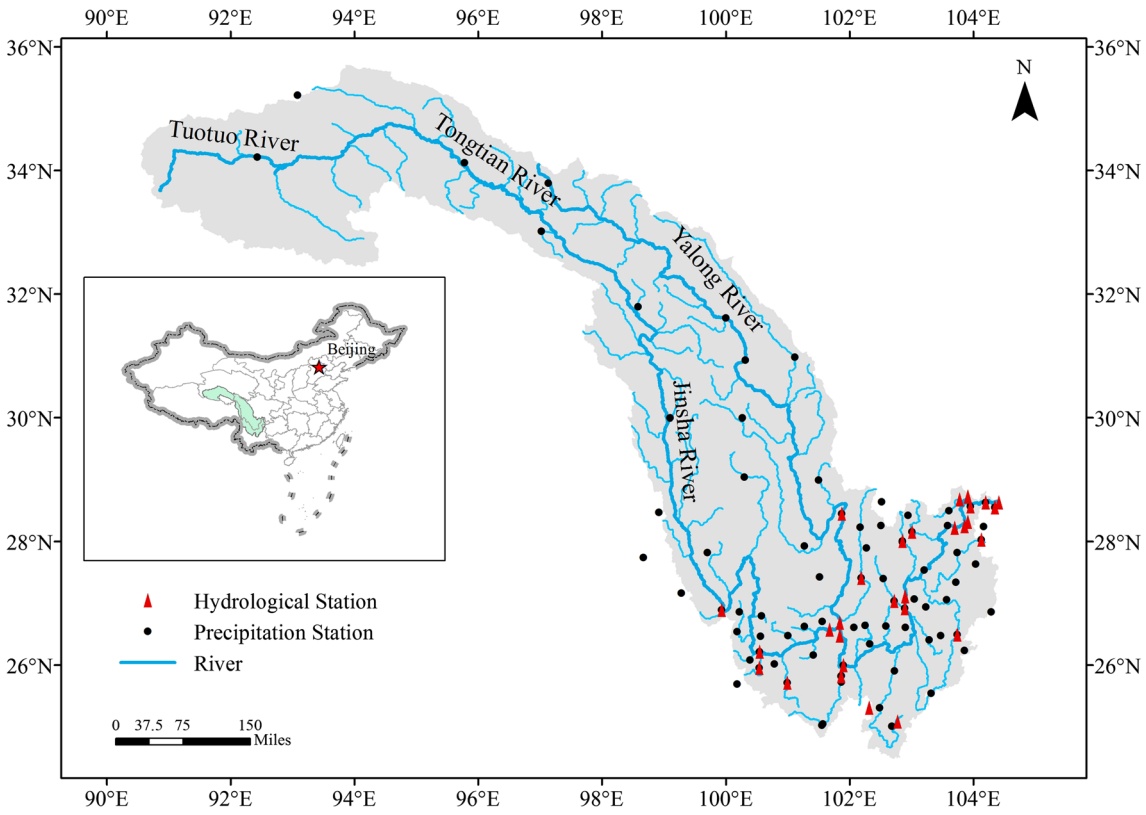

Fig. 1 Geographical location of the Jinshajiang River Basin in China

Kunming quasi-stationary front and the southwest air current, which causes overcast and rainy weather. In the summer half year (June through September or May through October), the westerly zone retreats to the north and there is abundant precipitation in the basin, which is primarily influenced by the maritime southwest and southeast monsoons. The precipitation gradually decreases from the southeast to the northwest.

The mean annual precipitation in the Jinshajiang River Basin is approximately 756.4 mm. However, the precipitation has noticeable seasonal and regional variations, with higher precipitation in the lower reaches of the basin than in the upper reaches. The precipitation reaches its peak in the summer season. The mean annual river discharge at the hydrological station Xiangjiaba, which is located at the lower reaches of the basin, is approximately 4610 m^3/s. The river discharge through a year has a single-peak distribution, and its highest levels occur between July and September, a month after the annual precipitation peak. Figure 1 shows the geographical location of the Jinshajiang River Basin in China.

2.2 Data

To analyze the precipitation simulation effects of the WRF model in the Jinshajiang River Basin, the observed precipitation data from the 60 monitoring stations were used in this study. The daily observed precipitation data (from January 1, 1961 to December 31, 2013) of the Jinshajiang River Basin and its 32 surrounding national standard meteorological stations were used. The data were provided by the Climate Data Center of the National Meteorological Information Center of China Meteorological Administration. In addition to the data from the 32 national standard meteorological stations, the observed precipitation data from 28 precipitation stations within the basin (data taken from the precipitation monitoring network in the basin) were also used.

To establish the hydrological model with 1-h forecast accuracy, the observed hourly runoff data (from January 1 2004 to December 31 2013) of the 17 control stations (such as Xiangjiaba station, Xiluodu station et al.) in the Jinshajiang River Basin were used for calibration and validation of the hydrological model. We naturalized the runoff data at the beginning to remove the storage effects of the upper hydropower stations. Furthermore, Zhang et al. (2007) showed that the runoff data over the 45 years only have a very slight downward tendency which is not remarkable. Therefore, the consistency of the calibration and validation was guaranteed. Figure 1 also shows the distribution of the precipitation stations and the runoff stations within the Jinshajiang River Basin and surrounding areas.

3 Research methods

3.1 WRF model for precipitation simulation and prediction

The WRF model is a numerical weather prediction system designed for atmospheric research and weather forecasting and was collectively developed by a number of US research and development organizations, including the National Center for Atmospheric Research, the National Oceanic and Atmospheric Administration, the Forecast Systems Laboratory, and the Center for Analysis and Prediction of Storms of University of Oklahoma (Jankov et al. 2005; Skamarock et al. 2005).

In this study, the WRF was used to establish the numerical weather model for simulating precipitation in the Jinshajiang River Basin. A non-hydrostatic, fully compressible Euler equation was adopted as the dynamic framework. The terrain-following hydrostatic-pressure coordinate was used as the vertical coordinate, and the variables were staggered in the horizontal Arakawa C-grid. The time scheme was the third-order Runge–Kutta. In the vertical direction, η area was used and divided into 27 layers. Based on the weather and climate characteristics of the Jinshajiang River, the rapid radiative transfer model (RRTM) scheme was adopted as the long-wave radiation scheme; the Goddard scheme was used as the short-wave radiation scheme; the Eta similarity scheme was used as the surface layer scheme; and the Noah scheme was used as the land surface process scheme. The 1.0 × 1.0 degree global tropospheric final (FNL) data provided by National Centers for Environmental Prediction (NCEP) were used to generate the initial field and lateral boundary conditions.

3.2 Experiment scheme design of the WRF model

To select a proper combination of parameterization schemes for the WRF model, various combinations of the parameterization schemes were analyzed against their precipitation simulation results. Since the selection of parameterization schemes had a great impact on the precipitation simulation, various combinations of the cloud microphysics, boundary layer, and cumulus parameterization schemes were selected as candidates based on the physical meanings of different parameterization schemes of the WRF model and the precipitation characteristics of the Jinshajiang River Basin. The impact of different schemes in WRF on the precipitation simulation in the Jinshajiang River Basin was analyzed.

Furthermore, for the regional domain configuration, there are a number of nesting techniques available in the WRF model, where non-nesting modes can also be used. To select a proper regional nesting configuration for the WRF model, the results from the numerical model using both non-nesting and double regional nesting modes were analyzed, respectively.

3.3 Assessment method for precipitation simulations of the WRF model

Threat score (TS) was used to assess the effects of simulated precipitation using the WRF model and is defined as follows: A_c is the number of stations where precipitation is correctly simulated; A_f is the number of stations where simulated precipitation appears with no observed precipitation; A_0 is the number of stations where precipitation occurs in reality but is not simulated. The statistical value of TS is calculated using the equation below:

$$T_s = \frac{A_c}{A_f + A_o - A_c}. \quad (1)$$

Therefore, TS only reflects the success ratio when there is precipitation. T_s equals 1 when the simulated and observed precipitation areas completely overlap each other, indicating a correct simulation. In addition, the closer T_s gets to 0, the worse the simulation becomes. In the present study, TS was only used to assess light and heavier precipitation events. The light rain is defined as 0.1–10 mm.

3.4 Hydrological modeling

For a large area like Jinshajiang River Basin, its lack of historical data makes the distributed hydrological model inappropriate considering its computational efficiency and accuracy. Nevertheless, the lumped hydrological model is also not a suitable choice as it cannot distinguish the difference between sub-basins on their properties of runoff generation and flow routing. Therefore, we took a balanced approach that divided the Jinshajiang River Basin into several sub-basins and developed hydrological model, respectively. The Xinanjiang model, which has proven to be very effective in humid areas, is adopted in this study for runoff generation. The Muskingum channel routing method is adopted for flow routing to obtain hydrographs at specific locations of a basin.

More specifically, the Jinshajiang River Basin is divided into several sub-basins according to hydrological stations and the DEM data, and the runoff generating and routing calculation is conducted on sub-basin to get its runoff in the outlet. Then, we can conduct the flood routing from the channel down the outlet, thus acquiring the runoff process of the sub-basin's outlet. By summing up the outflow process of every sub-basin, we are able to get the outflow process of the whole basin. Taking the main control stations in Jinshajiang River Basin as the nodes in dividing its sub-basin, the result is shown as Fig. 2.

The main stream and tributary stream of the basin should be classified before the forecasting calculation. The short-term forecast for both main stream and tributary stream is calculated as follows: (1) for every tributary forecast section, the precipitation-runoff process is calculated using the Xinanjiang model, and then, we can get the runoff forecasting of this basin; (2) for every main stream forecast section, the runoff forecast starts from the upper boundary of its basin, forecasting the runoff for every tributary section towards downstream until it reaches the main stream section. The runoff forecasting for every main stream section consists of three parts: calculating the upstream main stream runoff that enters this main stream area using the Muskingum channel routing method, acquiring the precipitation-runoff for the area using the Xinanjiang model, and shifting the tributary flow that enters this area. By summing up the results of three parts, we can get the section runoff of the main stream forecast.

4 Application

We examine the parameterization and nesting mode of the WRF model over the Jinshajiang River Basin for four typical precipitation events first, and then establish the hydrological model after calibration and validation, and analyze the coupled hydro-meteorological system in the end.

4.1 Parameterization and nesting mode of the WRF model

4.1.1 Configuration of the combinations of parameterization schemes and nesting mode

In this study, five cloud microphysics schemes, three boundary layer schemes and three cumulus parameterization schemes were used. Therefore, 45 ($5 \times 3 \times 3 = 45$) different combinations of different schemes were created as candidates for the parameterization scheme collection. The scheme options for microphysical processes included the Kessler scheme, the Lin et al. scheme, the WRF single-moment 3-class scheme, the WRF single-moment 5-class scheme, and the Ferrier (new Eta) scheme. The scheme options for boundary layers included the YSU scheme, the Mellor–Yamada–Janjic (Eta) TKE scheme, and the ACM2 (Pleim) scheme. In addition, the Kain–Fritsch (new Eta) scheme, the Betts–Miller–Janjic scheme, and the Grell–Devenyi ensemble scheme were the scheme options for cumulus parameterization. Considering the weather and climate characteristics of the Jinshajiang River Basin, the effect of snow cover was not taken into

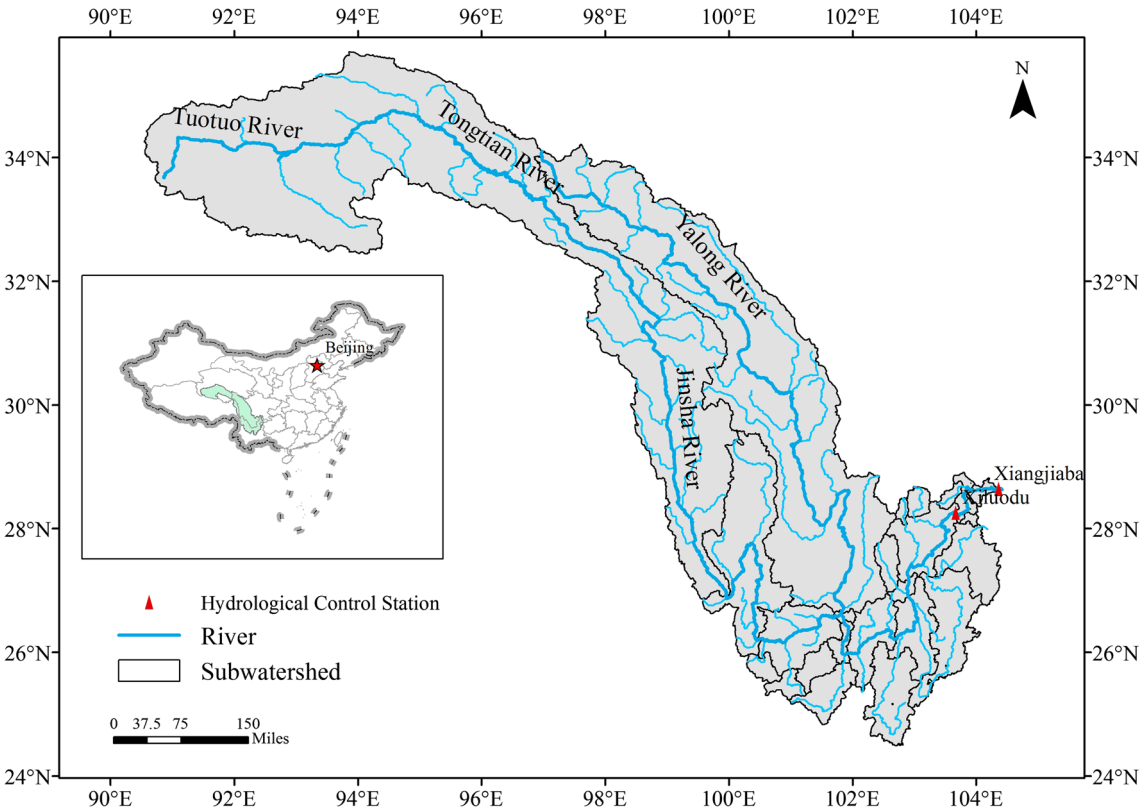

Fig. 2 Sub-basins of the Jinshajiang River Basin

account in the WRF model. Table 1 lists the 45 candidate combinations of the parameterization schemes.

To select a proper regional nesting configuration for the WRF model, we testified both non-nesting and double regional nesting modes. In the non-nesting mode, the coordinate of the central point was 29.21°N and 99.08°E, and a Lambert projection was used as the projection mode. The horizontal resolution was 10 km, whereas the grid number was 349 × 236. In the double regional nesting mode, the coordinates of the central point of both the rough and fine domains were 30.45°N and 96.60°E, and a Lambert projection was also used as the projection mode. The horizontal resolutions of the rough and fine domains were 30 and 10 km, respectively, and the grid numbers of the rough and fine domains were 103 × 66 and 247 × 166, respectively.

4.1.2 Typical precipitation processes

To maintain consistency with the timeframe of the NCEP-FNL data, the observed precipitation data from 1999 to 2010 in the Jinshajiang River Basin were used for analysis. Four typical precipitation events with the highest daily precipitation during 1999–2010 were selected for the simulation. All four precipitation events occurred in the main rainy season, and the dates of their occurrence were 28th Jul, 2001, 9th Aug, 2002, 6th Jun, 2003, and 20th Jul, 2007, respectively. The centers of the storms were primarily in the middle and the lower reaches of the Jinshajiang River Basin. Figure 3 shows the spatial distributions of the four typical precipitation events.

4.1.3 Initial selection of the combinations of parameterization schemes and nesting mode

1. Initial selection of the combinations of parameterization schemes
   To select the optimal combinations of parameterization schemes of the WRF model for the Jinshajiang River Basin, precipitation was simulated for the selected four typical precipitation events using 45 combinations of parameterization schemes by applying the non-nesting mode. TSs of the results of simulated precipitation for light and heavier rain using the 45 combinations of the schemes were calculated, and we selected six combinations with the highest TSs.
   Through the calculation of TSs, six combinations of the microphysics scheme, boundary layer scheme, and cumulus parameterization scheme with accurate simulation results were selected: ① the Lin et al. scheme, the YSU scheme, and Kain–Fritsch (new Eta) scheme combination (combination 1); ② the WRF single-moment 3-class scheme, YSU scheme and Kain–Fritsch (new Eta) scheme combination (combination 2); ③ the Lin et al. scheme, Mellor–Yamada–Janjic (Eta) TKE scheme, and Grell–Devenyi ensemble scheme combination (combination 3); ④ the Lin et al. scheme, Mellor–Yamada–Janjic (Eta) TKE scheme, and Kain–Fritsch (new Eta) scheme combination (combination 4); ⑤ the Lin et al. scheme, ACM2 (Pleim) scheme, and Kain–Fritsch (new Eta) scheme combination (combination 5); and ⑥ the Ferrier (new Eta) scheme, Mellor–Yamada–Janjic (Eta) TKE scheme, and Kain–Fritsch (new Eta) scheme combination (combination 6).
2. Comparison among different nesting modes
   To select the regional nesting mode for the WRF model, six parameterization combinations selected above were further studied. Both non-nesting and double nesting modes of the WRF model were applied to the six combinations, and simulations were carried out on the four typical precipitation events, with TSs calculated accordingly. Table 2 lists the TSs for light and heavier rain of the six combinations under different nesting modes.
   The results (Table 2) show that there was a little difference in the TSs of simulated precipitation for the four typical precipitation events when applying non-nesting or double nesting modes in the WRF model. Overall, non-nesting modes were slightly better than double nesting modes. Considering computing efficiency and structure simplification, the non-nesting mode of the WRF model was chosen in latter study.

4.1.4 Analysis of the optimum combinations of the parameterization schemes

As for the parameterization schemes used by the six combinations, the Kain–Fritsch (new Eta) scheme appeared most frequently as the cumulus parameterization scheme, which indicates that the selection of the cumulus parameterization scheme did not have the same impact on the precipitation simulation as the selection of the microphysics and boundary layer schemes did. In addition, the Kain–Fritsch (new Eta) scheme was relatively suitable for acting as the cumulus parameterization scheme for the region. The Kain–Fritsch (new Eta) scheme is an improved version of the Kain–Fritsch scheme. Using a simple cloud model with the ascending and sinking of moist air, the Kain–Fritsch (new Eta) scheme considers the influences from the entrapment of updrafts, the plume of downdrafts, and the relatively rough microphysical processes. This new scheme restricts large-range convection by considering the minimum entrainment rate in a dry environmental field with unstable edges. For updrafts that do not have a

Table 1 Forty-five candidate combinations of the parameterization schemes for the Jinshajiang River Basin

ID	Microphysical processes	Boundary layer	Cumulus parameterization
1	Kessler	YSU	Kain–Fritsch (new Eta)
2	Kessler	YSU	Betts–Miller–Janjic
3	Kessler	YSU	Simplified Arakawa–Schubert
4	Kessler	Mellor–Yamada–Janjic (Eta) TKE	Kain–Fritsch (new Eta)
5	Kessler	Mellor–Yamada–Janjic (Eta) TKE	Betts–Miller–Janjic
6	Kessler	Mellor–Yamada–Janjic (Eta) TKE	Simplified Arakawa–Schubert
7	Kessler	ACM2 (Pleim)	Kain–Fritsch (new Eta)
8	Kessler	ACM2 (Pleim)	Betts–Miller–Janjic
9	Kessler	ACM2 (Pleim)	Simplified Arakawa–Schubert
10	Lin et al.	YSU	Kain–Fritsch (new Eta)
11	Lin et al.	YSU	Betts–Miller–Janjic
12	Lin et al.	YSU	Simplified Arakawa–Schubert
13	Lin et al.	Mellor–Yamada–Janjic (Eta) TKE	Kain–Fritsch (new Eta)
14	Lin et al.	Mellor–Yamada–Janjic (Eta) TKE	Betts–Miller–Janjic
15	Lin et al.	Mellor–Yamada–Janjic (Eta) TKE	Simplified Arakawa–Schubert
16	Lin et al.	ACM2 (Pleim)	Kain–Fritsch (new Eta)
17	Lin et al.	ACM2 (Pleim)	Betts–Miller–Janjic
18	Lin et al.	ACM2 (Pleim)	Simplified Arakawa–Schubert
19	WRF single-moment 3-class	YSU	Kain–Fritsch (new Eta)
20	WRF single-moment 3-class	YSU	Betts–Miller–Janjic
21	WRF single-moment 3-class	YSU	Simplified Arakawa–Schubert
22	WRF single-moment 3-class	Mellor–Yamada–Janjic (Eta) TKE	Kain–Fritsch (new Eta)
23	WRF single-moment 3-class	Mellor–Yamada–Janjic (Eta) TKE	Betts–Miller–Janjic
24	WRF single-moment 3-class	Mellor–Yamada–Janjic (Eta) TKE	Simplified Arakawa–Schubert
25	WRF single-moment 3-class	ACM2 (Pleim)	Kain–Fritsch (new Eta)
26	WRF single-moment 3-class	ACM2 (Pleim)	Betts–Miller–Janjic
27	WRF single-moment 3-class	ACM2 (Pleim)	Simplified Arakawa–Schubert
28	WRF single-moment 5-class	YSU	Kain–Fritsch (new Eta)
29	WRF single-moment 5-class	YSU	Betts–Miller–Janjic
30	WRF single-moment 5-class	YSU	Simplified Arakawa–Schubert
31	WRF single-moment 5-class	Mellor–Yamada–Janjic (Eta) TKE	Kain–Fritsch (new Eta)
32	WRF single-moment 5-class	Mellor–Yamada–Janjic (Eta) TKE	Betts–Miller–Janjic
33	WRF single-moment 5-class	Mellor–Yamada–Janjic (Eta) TKE	Simplified Arakawa–Schubert
34	WRF single-moment 5-class	ACM2 (Pleim)	Kain–Fritsch (new Eta)
35	WRF single-moment 5-class	ACM2 (Pleim)	Betts–Miller–Janjic
36	WRF single-moment 5-class	ACM2 (Pleim)	Simplified Arakawa–Schubert
37	Ferrier (new Eta)	YSU	Kain–Fritsch (new Eta)
38	Ferrier (new Eta)	YSU	Betts–Miller–Janjic
39	Ferrier (new Eta)	YSU	Simplified Arakawa–Schubert
40	Ferrier (new Eta)	Mellor–Yamada–Janjic (Eta) TKE	Kain–Fritsch (new Eta)
41	Ferrier (new Eta)	Mellor–Yamada–Janjic (Eta) TKE	Betts–Miller–Janjic
42	Ferrier (new Eta)	Mellor–Yamada–Janjic (Eta) TKE	Simplified Arakawa–Schubert
43	Ferrier (new Eta)	ACM2 (Pleim)	Kain–Fritsch (new Eta)
44	Ferrier (new Eta)	ACM2 (Pleim)	Betts–Miller–Janjic
45	Ferrier (new Eta)	ACM2 (Pleim)	Simplified Arakawa-Schubert

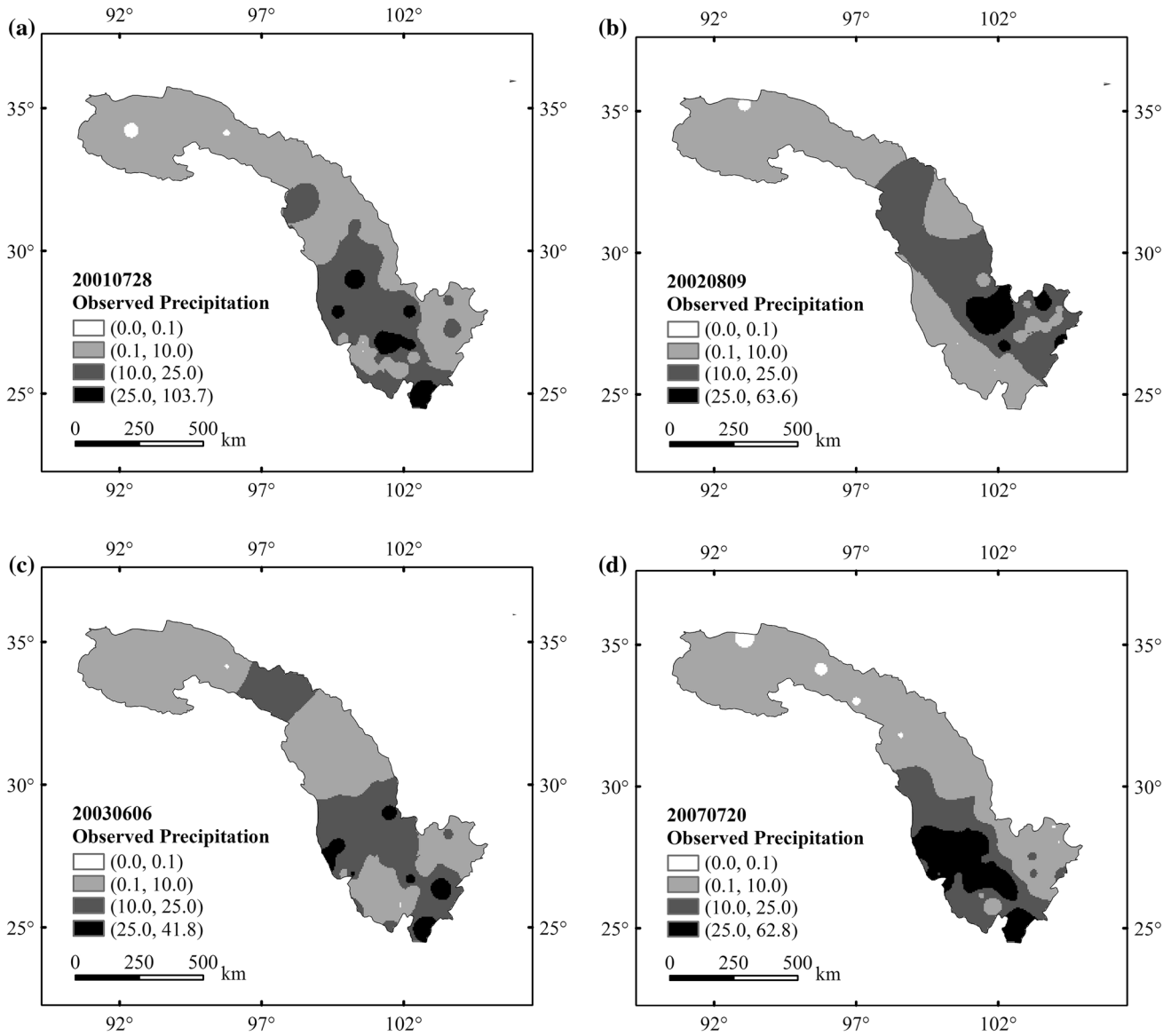

Fig. 3 Spatial distributions of the four typical precipitation events

Table 2 TS of accumulated light rain grades under different nesting modes for six combinations

Precipitation events	Nesting frameworks	Combination					
		1	2	3	4	5	6
28th Jul 2001	Non-nesting	0.857	0.896	0.898	0.898	0.896	0.898
	Double nesting	0.875	0.875	0.878	0.878	0.854	0.878
9th August 2002	Non-nesting	0.936	0.936	0.896	0.917	0.957	0.915
	Double nesting	0.915	0.915	0.915	0.917	0.915	0.915
6th June 2003	Non-nesting	0.936	0.957	0.936	0.936	0.936	0.956
	Double nesting	0.915	0.957	0.936	0.936	0.936	0.935
20th July 2007	Non-nesting	0.946	0.930	0.946	0.930	0.929	0.946
	Double nesting	0.930	0.930	0.878	0.860	0.929	0.911

minimum precipitation cloud thickness, the scheme considers shallow convection. The minimum precipitation cloud thickness changes with the cloud base temperature (Kain and Fritsch 1993).

The results from the simulation on the four typical precipitation events show that the selection of the cloud microphysics and boundary layer schemes has the highest impact on the precipitation simulation in the Jinshajiang River Basin. A proper combination of the cloud microphysics and boundary layer schemes could help to improve the precision of precipitation simulation. Meanwhile, the simulation results from combinations 3 and 5 were slightly better than the other combinations. In these two combinations, the Lin et al. scheme was used as the cloud microphysics scheme. The Lin et al. scheme was also used in other combinations, such as combinations 1 and 4. The Lin et al. scheme includes a predication for moist air, cloud water, rain, cloud ice, snow, and graupel. When the temperature is below freezing point, the cloud water is treated as cloud ice, where rain is treated as snow. The Lin et al. scheme is a relatively mature scheme in the WRF model.

By simulating basic conditions that directly influence the occurrence of storms, and then further simulating the regional occurrence and precipitation intensity of a storm, the cloud microphysical parameterization scheme plays a major and sensitive role in storm simulation. However, it is also worth noticing that the boundary layer scheme also has a great impact on precipitation simulation. For instance, the boundary layer scheme was different in combinations 3 and 5, which indicates that the precipitation simulated using the WRF model could only be consistent with the spatial distribution pattern of the observed precipitation when the combination of the three schemes were able to properly simulate precipitation events in the Jinshajiang River Basin. In addition, because of the differences among precipitation events in terms of their dynamic characteristics (e.g., cloud microphysics), using the mesoscale model to simulate regional storms is a complex process. For each individual precipitation event, it may be necessary to use different combinations of parameterization schemes for simulation and analysis.

4.2 Establishment of the hydrological model

Using the data of 2004–2009 as calibration period, we calibrate the Xinanjiang model in every mainstream section taking determinacy coefficient as objective function. After calibration, the data of 2010–2013 are adopted as validation period, and we examined the performance of these constructed models in every mainstream section as well. The calibration algorithm adopted is Shuffled Complex Evolution (SCE) algorithm. The detail of the Xinanjiang Model and SCE algorithm can be found in Ren-Jun (1992), Duan et al. (1994) and Kang and Lee (2014). The determinacy coefficients of calibration and validation period for 7 mainstream sections are shown in Table 3.

Table 3 Determinacy coefficients of calibration and validation period for seven mainstream sections

ID	Mainstream section	Determinacy coefficient	
		Calibration	Validation
1	Panzhihua–Sanduizi	0.980	0.990
2	Sanduizi–Longjie	0.986	0.980
3	Longjie–Wudongde	0.991	0.988
4	Wudongde–Huatan	0.946	0.927
5	Huatan–Baihetan	0.910	0.915
6	Baihetan–Xiluodu	0.820	0.858
7	Xiluodu–Xiangjiaba	0.976	0.912

From the table, we can see that the hydrological models constructed for every mainstream section performed well in both calibration and validation period, which can provide a high reliability in flood forecasting.

4.3 Experiment results and analysis of the flood forecast system

4.3.1 Precipitation forecast

To compare with the WRF mode, the precipitation forecast between 2012 and 2013 of meteorological center in Cascade Dispatching Center of China Three Gorges Corporation is introduced here. Because of the construction of Xiluodu Dam, the regulating and storage function of Xiluodu reservoir altered the original basin precipitation-runoff process and made the runoff forecast of Xiangjiaba inaccurate. Therefore, in this study, Xiluodu station is selected as analysis site instead of Xiangjiaba. Sixty-nine precipitation events were selected between 2012 and 2013 to compare forecasts precision between the WRF model and meteorological center.

For the 69 precipitation events in Baihetan–Xiluodu section, the precipitation forecast performances of the WRF model and Meteorological Center in given time interval (including 0–12 h, 12–24 h, and 24–36 h) are shown in Fig. 4.

As can be seen from the figure, the precipitation forecast by the WRF model does describe the precipitation process as it actually occurred, but the forecast value is bigger than the observed value sometimes. This is consistent with the result in Sect. 4, that the WRF model has a better performance for light and heavier precipitation. For the forecast period of 12–24 h, there are extreme precipitations that neither WRF nor Meteorological Center has characterized.

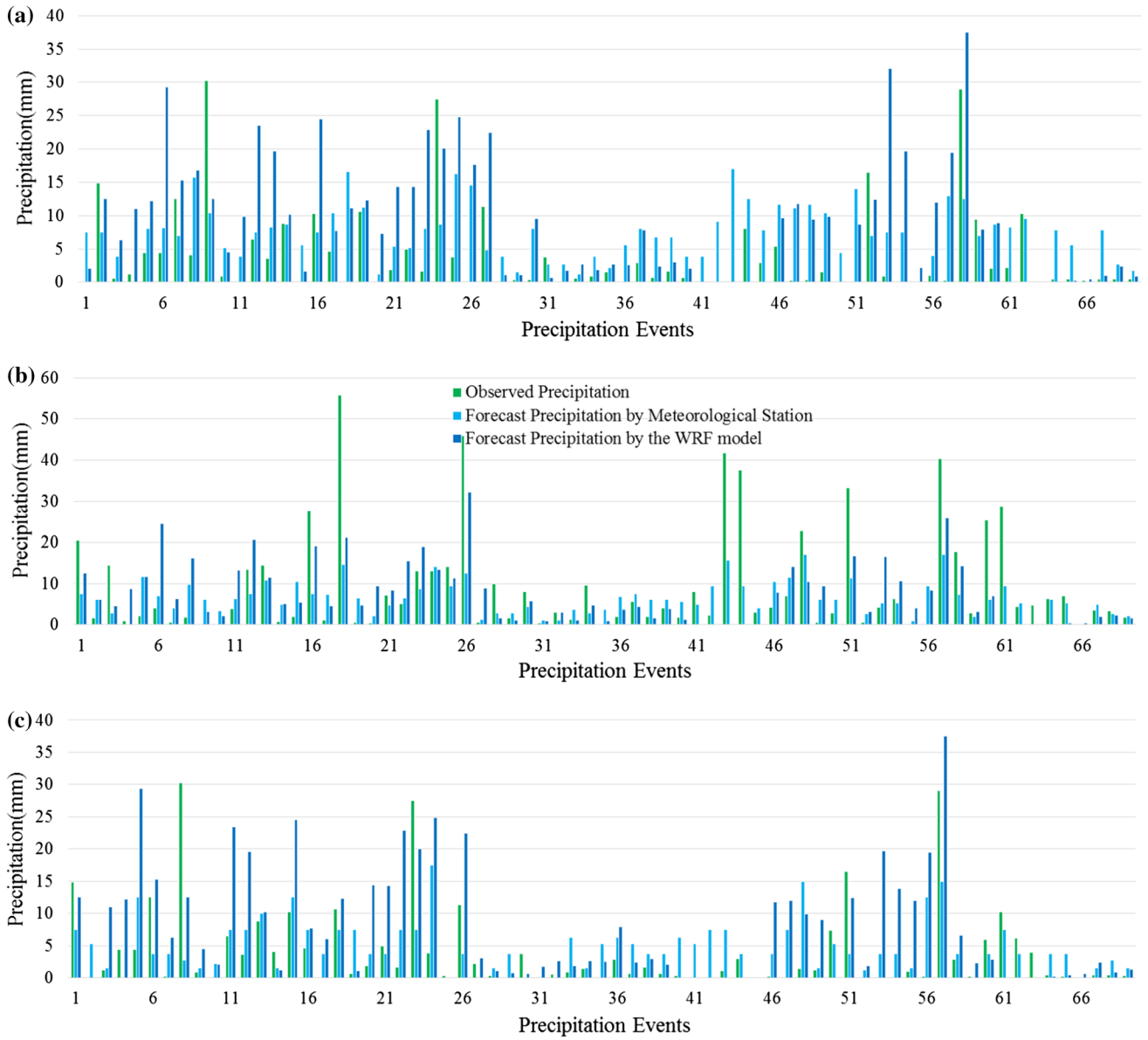

Fig. 4 Precipitation forecast performances of the WRF model and Meteorological Center in 0–12 h (**a**), 12–24 (**b**), and 24–36 (**c**)

However, for the forecast periods of 0–12 h and 24–36 h, the precipitation forecasts using the WRF model may have a better performance.

4.3.2 Real-time flood forecasts of coupled hydro-meteorological system

In this study, the flood forecasting lead time is increased by 36 h at least as the precipitation forecast introduced here. Figure 5 shows the relative errors of the forecast floods on three precipitation inputs including the WRF model, Meteorological Center, and observed value for the 69 precipitation events in the Baihetan–Xiluodu section in given time interval (including 0–12 h, 12–24 h, 24–36 h).

According to Fig. 5, the relative errors of the forecast floods on three precipitation inputs (precipitation forecast by the WRF model, precipitation forecast by Meteorological Center, and observed precipitation) are consistent on the whole, and it indicates that the precipitation forecast using the WRF model has the ability to reflect reality and can be used as a guidance in the practical production of hydropower system.

Comparing the flood forecasted by the precipitation of the WRF model with the others, the former is somewhat bigger than the latter, because the precipitation forecasted by the WRF model is bigger than others, which is verified before. For some flood events, even the observed precipitation is bigger than the WRF model's forecast

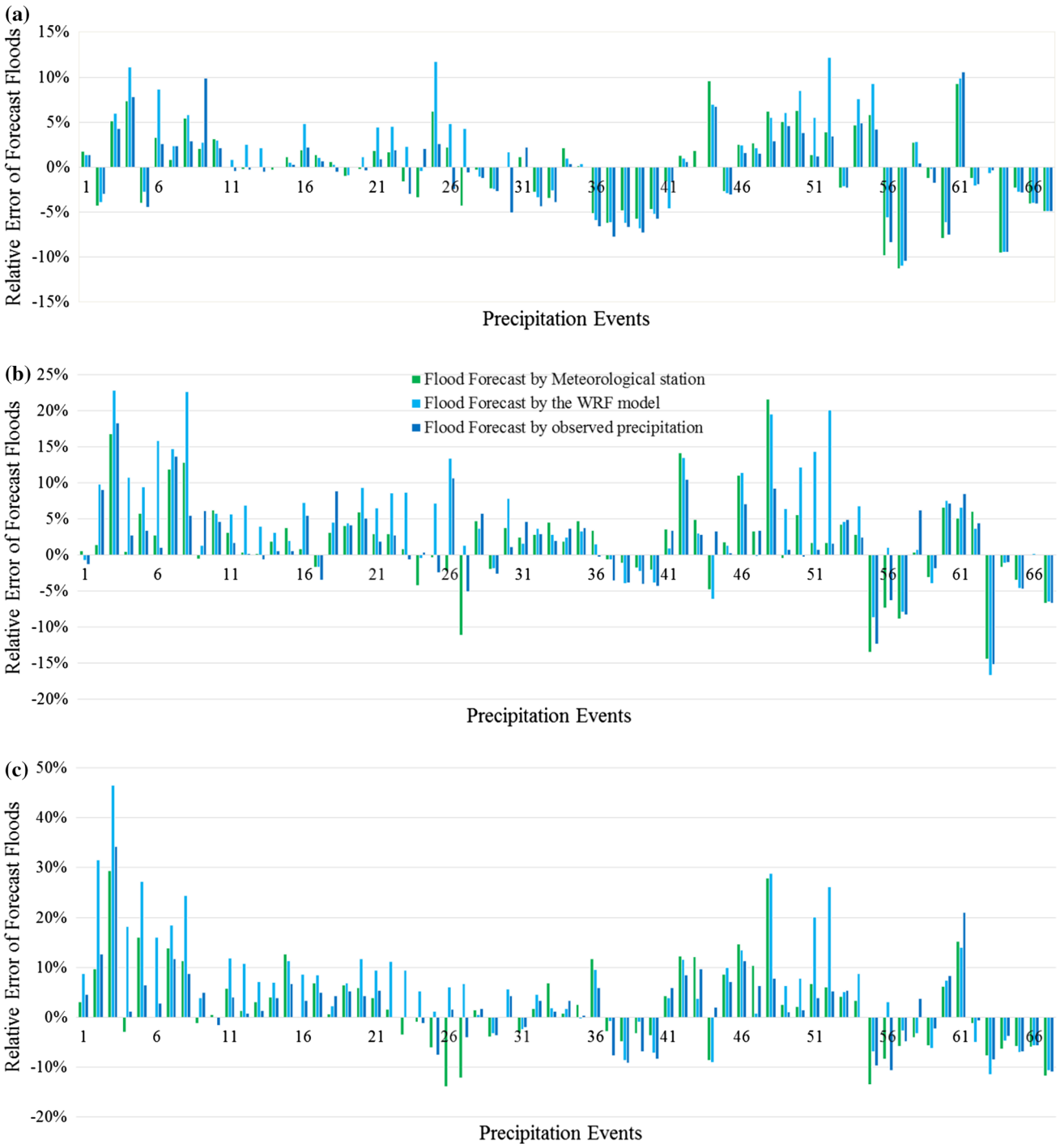

Fig. 5 Relative errors of the forecast floods on three precipitation inputs in 0–12 h (**a**), 12–24 h (**b**), and 24–36 h (**c**)

precipitation, but when it comes to the hydrograph evaluation, the forecast flood by observed precipitation is smaller than the WRF model. The reason is that the flood is forecasted from upstream to downstream in the flood forecast system, instead of using the precipitation forecast of Baihetan–Xiluodu section only, the precipitation forecasts of all the other sections are used here. Even though the precipitation forecast of Baihetan–Xiluodu section is smaller than observed precipitation, the other sections' precipitation forecasts may be larger than observed.

For the flood events whose flood amount is huge, the forecast flood using the WRF model's precipitation as input has better performance than others. It is because of the big flood events, the floods coming from Panzhihua and

Tongzilin take up the majority of the forecast flood as section's precipitation-runoff process counts little. On the contrary, for those flood events whose amount is smaller, the forecast flood by the WRF model's precipitation is sometimes bigger than others, because the section's precipitation-runoff process takes majority of the forecast flood which may be forecasted larger by big precipitation forecast by the WRF model.

5 Results and discussion

In this study, the combinations of the parameterization schemes of the mesoscale weather model suitable for precipitation simulation in the Jinshajiang River Basin (the largest hydropower base in China) were first investigated. There are a number of factors that can influence precipitation in the Jinshajiang River Basin, including topography, geographical location, atmospheric circulation, and characteristics of underlying surface. Hence, the spatial variation of the precipitation is relatively large, and the spatial distribution of the precipitation is uneven. Therefore, to describe the precipitation characteristics, the proper combinations of parameterization schemes in the WRF model were investigated.

The mesoscale weather model, WRF, was used in the present study for the precipitation simulation for four typical rainy season precipitation events in the Jinshajiang River Basin. Combinations of the microphysics scheme, boundary layer scheme, and cumulus parameterization scheme were optimized to select mode structures of the WRF model. Together, 45 different combinations of parameterization schemes were used for the simulation of the four typical precipitation events, which were subsequently assessed using the TS.

Our results show that the selection of the cloud microphysics and boundary layer schemes had a significant impact on the precipitation simulation in the Jinshajiang River Basin and that only a proper combination of these two schemes could yield satisfactory simulation results. For the precipitation simulation in the Jinshajiang River Basin, the Lin et al. scheme was the preferred choice for the cloud microphysics scheme. However, the selection of the cloud microphysics scheme should also be compatible with the selection of the boundary layer scheme, as the boundary layer scheme also plays an important role in precipitation simulation. Our study shows that when the Mellor–Yamada–Janjic (Eta) TKE scheme or ACM2 (Pleim) scheme was used as the boundary layer scheme, the Lin et al. scheme could be used as the compatible cloud microphysics scheme to generate satisfactory simulation results. The selection of the cumulus parameterization scheme did not have the same degree of impact on precipitation simulation of the WRF model as the other two schemes. The Kain–Fritsch (new Eta) scheme was relatively suitable to be used as the cumulus parameterization scheme for this region.

In addition, both non-nesting and double nesting modes were used in the WRF model for precipitation simulation. The TSs for light and heavier rain showed that the simulation with the double nesting mode was not more accurate than with the non-nesting mode. For the four typical precipitation events, the simulation results generated using the non-nesting mode with a lattice horizontal resolution of 10 km were not significantly different from the simulation results generated from the double nesting mode. Overall, the simulation results generated using the non-nesting mode were slightly better than those using the double nesting mode.

The results show that the WRF model could be used for precipitation simulation and prediction in the Jinshajiang River Basin for light and heavier rain, because those TSs were generally over 0.85. However, the precision of simulation for moderate rain, especially heavy rain or storms, was relatively poor.

On the basis of the WRF model for precipitation in the Jinshajiang River Basin, a flood forecast system from upstream to downstream was built. Based on the DEM and the runoff stations in the Jinshajiang River Basin, the basin was divided into seven sub-basins. For every sub-basin, its forecast runoff consists of three parts: the river flood routing which enters from its upper boundary, the precipitation-runoff process for the mainstream subinterval, and the runoff from tributary streams after shifting them for their transform hours. Then, comparisons between observed precipitation and forecast precipitation from the WRF model and forecast precipitation from Meteorological Center of China Three Gorges Corporation were made, so are their performance when used as the input for the flood forecast system. The results show that the WRF model can describe the precipitation process with a little overestimation sometimes. When used as the input of the flood forecast system, it also achieved a good performance, which allows it to be used in hydrological forecasting operations to increase real-time flood forecasting lead time.

In summary, the optimum combinations of the parameterization schemes and mode structures of the WRF model were suitable for precipitation simulations and predictions in the Jinshajiang River Basin can be used as the input of the flood system to provide a forecast flood with high precision. However, it is also worth noticing that only four typical precipitation events were selected for simulation, which is not an integrated representative of the precipitation characteristics of the Jinshajiang River Basin. Therefore, further investigation on additional precipitation events is required. Moreover, the ensemble prediction of different

combinations of parameterization schemes of the WRF model should also be further investigated.

Acknowledgements This work is supported by the Key Program of the Major Research Plan of the National Natural Science Foundation of China (No. 91547208), the National Natural Science Foundation of China (No. 51579107), and the National Key R&D Program of China (2016YFC0402205 and 2016YFC0402209).

References

Deb SK, Srivastava TP, Kishtawal CM (2008) The WRF model performance for the simulation of heavy precipitating events over Ahmadabad during August 2006. J Earth Syst Sci 117(5):589–602

Duan Q, Sorooshian S, Gupta VK (1994) Optimal use of the SCE-UA global optimization method for calibrating watershed models. J Hydrol 158(3):265–284

Gilliam RC, Pleim JE (2010) Performance assessment of new land surface and planetary boundary layer physics in the WRF-ARW. J Appl Meteorol Clim 49(4):760–774

He M, Zheng H, Huang X, Jia J, Li L (2013) Yangtze River sediments from source to sink traced with clay mineralogy. J Asian Earth Sci 69:60–69

Hong S, Dudhia J, Chen S (2004) A revised approach to ice microphysical processes for the bulk parameterization of clouds and precipitation. Mon Weather Rev 132(1):103–120

Jankov I, Gallus WA Jr, Segal M, Shaw B, Koch SE (2005) The impact of different WRF model physical parameterizations and their interactions on warm season MCS rainfall. Weather Forecast 20(6):1048–1060

Kain JS, Fritsch JM (1993) Convective parameterization for mesoscale models: The Kain–Fritsch scheme. The representation of cumulus convection in numerical models. Springer, New York, pp 165–170 **(reprinted)**

Kang T, Lee S (2014) Modification of the SCE-UA to include constraints by embedding an adaptive penalty function and application: application approach. Water Resour Manag 28(8):2145–2159

Raju P, Potty J, Mohanty UC (2011) Sensitivity of physical parameterizations on prediction of tropical cyclone Nargis over the Bay of Bengal using WRF model. Meteorol Atmos Phys 113(3–4):125–137

Skamarock WC, Klemp JB, Dudhia J, Gill DO, Barker DM, Wang W, Powers JG (2005) A Description of the Advanced Research WRF Version 2. Report No. NCAR/TN 468+STR

Srivastava PK, Islam T, Gupta M, Petropoulos G, Dai Q (2015) WRF dynamical downscaling and bias correction schemes for NCEP estimated hydro-meteorological variables. Water Resour Manag 29(7):2267–2284

Wu W, Xu S, Lu H, Yang J, Yin H, Liu W (2011) Mineralogy, major and trace element geochemistry of riverbed sediments in the headwaters of the Yangtze, Tongtian River and Jinsha River. J Asian Earth Sci 40(2):611–621

Yuan X, Liang X, Wood EF (2012) WRF ensemble downscaling seasonal forecasts of China winter precipitation during 1982–2008. Clim Dynam 39(7–8):2041–2058

Zeng X, Wu Z, Xiong S, Song S, Zheng Y, Liu H (2011) Sensitivity of simulated short-range high-temperature weather to land surface schemes by WRF. Sci Chin Earth Sci 54(4):581–590

Zhang J et al (2007) Study of runoff of the six large basins in China over the past 50 years. Adv Water Sci 2:230–234 **(in Chinese)**